SCALING EFFECTS ON RUNOFF AND SOIL MOISTURE CONTENT IN A GIS-BASED, VARIABLE-SOURCE-AREA HYDROLOGY MODEL

Wen-Ling Kuo, Tammo S. Steenhuis, Charles E. McCulloch, Charles L. Mohler,
David Weinstein, Stephen DeGloria, and Dennis Swaney

May 1, 1998

ABSTRACT

Recent research on soil chemical and biological dynamics in mixed use landscapes has shown that the distributions of soil moisture and water transport are crucial for environmental management. In this paper, we examine the effect of scaling on soil water content for a grid based, spatially explicit, variable-source-area hydrology model in a watershed in central New York. Data on topography, soil type and land use were input at grid sizes from 10 to 600 m. Output data consisted of runoff and spatial pattern of soil moisture. Simulation results showed higher average soil water contents for large grid sizes, because curvature of the land and (to a lesser degree) slope gradient decreased with increasing grid size. Higher moisture contents, in turn, increased evaporation and slightly decreased the runoff. Larger grid sizes also decreased the spatial variability of moisture content, especially, during dry periods. Scaling did not affect the spatial distribution of land use and soil type. The results have ramifications for water quantity and quality simulations in watersheds with relatively shallow soils where runoff is generated by variable source area processes.

1. INTRODUCTION

In recent reports to the Congress of the United States of America [e.g., USEPA, 1994, 1995], the U.S. Environmental Protection Agency (USEPA) and many state water resource professionals agree that water quality management to address non-point source and habitat degradation problems must be at the basin or watershed level. This watershed approach will not only save time and money but may also achieve better environmental results [USEPA, 1996]. However, because it is difficult to design and perform experiments in a large watershed, research using spatially explicit models to simulate ecosystem processes has become increasingly important. This is especially true for watersheds in which shallow and sloping soils predominate, and the traditional approach using spatially averaged parameters is unable to describe the variation in water and nutrient fluxes in the watershed [Steenhuis et al., 1995; Swaney et al., 1996; Fisher et al., 1997].

Spatial dynamics of many biological and chemical processes are strongly affected by soil water content. Simulating water content and water flows in watersheds is, thus, of fundamental importance [Haith and Shoemaker, 1987]. In this paper, we investigate well-vegetated watersheds in the northeastern USA for which the hydraulic conductivity of soils exceeds rainfall intensity by several fold. Most soils in these watersheds have a shallow depth to an impermeable layer, and overland flow is generated from areas that become saturated during a rainstorm. Also, evaporation and interflow (flow parallel with the impermeable layer) are important components in water balance calculations [Dunne, 1978].

Simulating water dynamics in these watersheds is often complicated by the need to incorporate a vast amount of spatial information, including topography, soil type and land use [Beven and Kirkby, 1979; Beven, 1986, 1995]. Most distributed models are, thus, developed in a grid-based structure to efficiently integrate data and computational routines. Geographic information systems (GIS) have been helpful in this process [Moore et. al., 1991; Burrough, 1996]. The most common grid sizes in GIS databases are those used by the U.S. Geological Survey (USGS): 30 m in the USA and 50 m in the United Kingdom [Quinn et al., 1991; Moore et al., 1993].

A few studies have examined the effect of grid size on watershed simulations. Using TOPMODEL, Quinn et al. [1991], Moore et al. [1993], Zhang and Montgomery [1994], Bruneau et al. [1995], and Wolock and Price [1994] looked at how grid size affected the computed topographic characteristics, wetness index and outflow. In general, they found that the finer grid size gave more accurate results. TOPMODEL assumes that the downslope flows, take place predominantly in a saturated zone with a transmissivity that decreases with depth [Ambroise et al.,1996). In the northeastern US where variable source area hydrology is the main mechanism that generates surface runoff, saturated flow occurs only in shallow eroded soils a few hours after the rain ends [Steenhuis et al., 1988] and the assumption in TOPMODEL that flow takes place in the saturated soil does not apply. With the exception of the few studies with TOPMODEL, the effect of GIS grid size on watershed simulations has not been well investigated [Star and Estes, 1990; Star et al., 1997; Baveye, 1997]. Thus, the goal of this paper is to elucidate the role of scale in the simulation of water movement in a thin conductivity layer over an otherwise impermeable sloping subsoil.

In this paper, we use a GIS-based model that was specifically developed for undulating landscapes with a relatively thin conductive soil layer over glacial till that includes unsaturated flow [Zollweg et al., 1996; Kuo et al., 1996; Frankenberger et al., 1998]. Soil water movement and dynamics were simulated for three watersheds in upstate New York to evaluate the effect of scale on simulated soil water content and runoff was observed. The sensitivity of the model to aggregation was studied by factorially varying the grid size for different inputs. Information loss due to aggregation was calculated.

2. METHODS

2.1 Study site

Three adjacent watersheds (numbered 1, 2, and 3) of 647, 2360, and 742 ha, respectively, were chosen (Table 1, Fig. 1). They are typical for the northeastern USA. The watersheds are part of the Fall Creek Watershed and located upstream from Freeville, New York (N42°32', W76°17'). Terrain elevation ranges from 317 to 580 m, and slope gradient ranges from 0 to 60% (Table 1). Agriculture and forest are the main land uses. Annual precipitation averages 94 cm and mean annual air temperature 8.3°C [Owensby and Enzell, 1992]. Precipitation is nearly evenly distributed throughout the year. Most soils have a shallow depth to a layer that restricts water movement [Cornell University Department of Geology, 1959; Neeley, 1965].

Three digital maps were made for elevation, soil type, and land use using 10 m square grid cells. Elevation data were digitized from the contours of 1:24,000 USGS maps. Soil maps were obtained from soil surveys at 1:20,000 scale of Tompkins, Cortland, and Cayuga Counties. Land use information was interpreted from 1991 aerial photographs at 1:24,000 scale [Poiani et al., 1996].

2.2 The GIS-based hydrology model

The analysis was performed with a GIS-based model originally developed by Zollweg et al. [1996] and further improved by Kuo et al. [1996]. The model was designed for simulation of soil water and nitrogen fates in mixed use landscapes with sloping and shallow soils. The model was coded in shell script commands within the Geographic Resources Analysis Support System (GRASS) [CERL, 1993; Mitasova et al., 1995]. The simulations were performed using a daily time step.

Water balance equations were written to operate on a per grid cell basis and for each soil layer. The model divides the soil in two main layers: a potential root zone and the combination of several subsoil layers. The potential root zone is divided into the actual root zone (from which evaporation occurs) and the remaining part in which the roots can penetrate during the growing season. The change of soil water is calculated by combining Darcy's law and the conservation of mass equation, viz:

$$\frac{\partial \theta}{\partial t} = \nabla \cdot (K(\theta) \nabla h) + F(t) \qquad (1)$$

The first term of the right-hand side, $K(\theta)\nabla h$, takes into account the lateral exchange between cells where θ is the volumetric water content, h is the hydraulic head, and $K(\theta)$ is the hydraulic

conductivity as an exponential function of moisture content. ∇h is approximated by the change of elevation per unit length of grid in the downstream flow direction. The second term, F(t), expresses the vertical fluxes.

The function, F(t), uses the daily precipitation to determine the runoff, evaporation water loss to the atmosphere, and the water flux between the layers. Water flows downward at the rate of the saturated conductivity when the soil is above field capacity. If the layer below is filled up with water, downward movement stops. Local runoff occurs when the soil reaches saturation or precipitation intensity is greater than local saturated conductivity. Evapotranspiration takes place out of the active evaporation zone and is based on the Thornthwaite-Mather procedure [Steenhuis and van der Molen, 1986]. For moisture contents from field capacity to saturation, the evaporation is equal to the potential rate; and for moisture contents from field capacity to wilting point, evapotranspiration decreases linearly from a potential rate to zero. During the winter F(t) includes routines for snow accumulation and snowmelt.

Equation (1) can be rewritten as:

$$\frac{\partial \theta}{\partial t} = \frac{\partial K}{\partial \theta} \nabla \theta \, \nabla h + K \nabla^2 h + F(t) \qquad (2)$$

and then shows that the lateral exchange of water is a function of the first derivative (slope gradient) and the second derivative (the Laplacian) of the elevation. The Laplacian is related to the curvature of a landscape surface.

2.3 Spatial Aggregation

Increasing grid size results in a change in watershed area [Bruneau et al., 1995], and when comparing total runoff and average moisture content for different grid sizes, watershed area needs to be conserved. To do so, we calculated for each aggregated cell the proportion of 10 by 10 m cells (a_p) that was within the watershed. The fluxes of the aggregated border cells were then multiplied by this factor (a_p) ensuring that no water was gained through the scaling process. Figure 2 shows an example of spatial aggregation on a simple catchment from the small scale L = l to the larger scale L = 3 l. At the small scale, L = l, the catchment area, shown as gray color, is equal to 13 l^2. At the larger scale, L = 3 l, four coarse cells are within the catchment, and a $_p$ for those cells is 2/9, 2/9, 3/9, and 6/9, giving a value of 13/9 L^2. Because $L^2 = 9\,l^2$ the area is again equal to 13 l^2.

Based on the above discussion, Eq. (1) can then be written in finite difference form for cells with grid size, L, for a layer, i:

$$a_p D_i L^2 \frac{\Delta \theta_i}{\Delta t} = \Delta\left(\lambda D_i K(\theta) S\right) + a_p L^2 F_i(t) \tag{3}$$

$$\lambda = \sqrt{a_p L^2} \tag{4}$$

where, D_i is the depth of layer i. The term $\Delta(\lambda D_i K(\theta) S)$ is the net lateral flux of water and is computed as the product of the unsaturated conductivity, $K(\theta)$, slope, S, in the flow direction, and cross-sectional area, λD_i. Equation (4) shows, as expected, that for internal cells $\lambda = L$.

Another issue in aggregation was the value of the cell parameters. A distinction was made between continuous data (e.g., elevation) and categorical data (e.g., soil type and land use). For continuous data, the values of the component cells were averaged. For categorical data, the most common value of the component cells was selected. In case of a tie, one of the (equally) most common values was chosen at random. For border cells only the portion inside the watershed was considered.

2.4 Simulation experiment

The 10 x 10 m maps of elevation, soil type, land use, and watershed boundaries for the study area were aggregated to produce 14 sets of data with grid sizes of 10, 20, 30, 50, 70, 100, 120, 150, 170, 200, 300, 400, 500, and 600 m. The aggregated base maps were used to obtain the input maps for the simulation model (e.g., slope gradient and Laplacian from the elevation map, saturated conductivity from the soil map, and potential rooting depth from the land use map). A three-year simulation was performed by using the daily weather data from 4-1-91 to 3-31-93 obtained from the Northeast Regional Climate Center at Cornell University for Game Farm Road Station located in the Fall Creek Watershed. Year 0 (4-1-91 to 3-31-92) was used to set the initial moisture content of the cells. Year 1 consisted of the climate data for the period 4-1-92 to 3-31-93 (108 cm of precipitation). Year 2 consisted of the period 4-1-91 to 3-31-92 (82 cm of precipitation) used a second time.

2.5 Determination of dominant parameters -- factorial experiments

To determine the types of data for which grid size had the greatest effects on simulation output, we conducted two-factor simulation experiments [Neter et al., 1996]. Among input maps, we varied the scale of one map as a factor and varied all other maps simultaneously as the other factor. To compare the scaling effect on both factors, each factor had two spatial resolutions, 20 m and 200 m. Thus, four combinations of the factors were compared.

2.6 Information loss

The numerical values stored for each grid cell makes up the information of a map. Typically, as map resolution decreases (i.e., larger grid size), information is lost. To describe the effect of aggregation on the simulation results, we used the information (or entropy) theory by Shannon and Weaver [1949] which was introduced to hydrology by Vieux [1993] and Singh [1997].

For categorical data, such as land use, an information index (also called entropy), Ω, which represents a measure of variability of spatial information associated with an range of outcome values, is defined as:

$$\ln\Omega = -\sum_{i=1}^{N} P_i \ln(P_i) \tag{5}$$

where N is the number of categories (or bins) in the range into which the **categorical** values have been divided, and P_i is the proportion of cells of category i. Choices of range of outcome values and N are critical in comparing information indices over different scales

Choices of the bins for evaluating Ω for **continuous** data are more problematic. If the data were truly continuous, with an appropriate renormalization, N could be let to approach infinity. However, the GIS stores even "continuous" data as a discrete set and, consequently, when N is large, Ω approaches a value equal to the number of distinguishable values and becomes meaningless. A proper value for N has to be chosen. On one hand, we would like to have N large so that it reflects the fact that the data are continuous. On the other hand, we cannot choose N too large. For example, Figure 3 shows the Ω value of the slope and Laplacian versus N for maps of resolution 50, 200, and 600 m. Compromise values are evident from Fig. 3 and, hence, we chose N = 80 for quantifying information loss for slope gradient and N = 600 for the Laplacian.

3. RESULTS

3.1 Results from hydrological simulations

Simulated cumulative runoff, average monthly soil moisture, and cumulative effective precipitation over the three catchments are shown in Fig. 4. Soil moisture content is normalized from 0 to 1 where 0 is air dry soil and 1 is saturation. Effective precipitation is defined as the difference between rainfall and evapotranspiration. Soil moisture values (Fig. 4b) increased as the grid sizes increased. The

initial differences in moisture content (produced by the year 0 simulation) were approximately maintained throughout the two years, although differences were greatest during the dry summer of the second year (Figs. 4a and 4c). For larger grid sizes and higher average moisture contents, the cumulative effective precipitation and runoff became less over the two-year period. The higher moisture contents are directly related to an increase in actual evaporation and, thus, a lower effective precipitation. Runoff was the same for all the grid sizes during the wet year 1 (Fig. 4a) despite the difference in effective precipitation (Fig. 4c). Thus, the lower effective rainfall input for the larger grid sizes was offset by a smaller decrease in moisture content during the summer compared with the smaller grid sizes (which is confirmed by Fig. 4b). A similar argument can be made for the difference in cumulative runoff over the two-year period: Since, for the 400 m grid, the moisture content at the beginning and end of the simulation period was approximately the same (Fig. 4b), water balance considerations dictate that decreases in effective precipitation are directly related to a decrease in runoff from the watershed. Because the watershed becomes drier over the two-year period, the differences in runoff are not as great as the differences in effective precipitation.

The spatial distribution of soil moisture for a selected sample date, 3/31/93, at cell sizes of 10, 30, 50, 100, and 400 m is revealing (Fig. 5). This was the second day after a rain (0.83 cm precipitation), and there had been no rainfall or snowmelt for 5 days prior to the rain. In Fig. 5, darker regions represents drier soil and white color indicates soil near or at saturation. In the 10 m simulation, most areas were at field capacity, except areas near valley bottoms. The spatial pattern of the saturated areas indicated potential locations of flow channels and wetlands (white areas in Fig. 5). The pattern

of wetness also changed with grid size: The areas at field capacity on the 10 by 10 m grid in the middle of the figure became completely saturated ($\theta > 0.99\ \theta_s$) in the 400 m grid.

Although Fig. 5a is too small to see the many saturated individual 10 by 10 m grid cells, the overall pattern of wet areas shows a close correspondence with the poorly drained areas in Fig. 1. Poorly drained areas are defined in the Soil Survey as mostly wet throughout the year, but otherwise have the same hydraulic properties as similar soils in upland areas of the landscape. Thus, input parameters were the same for the wet and dry areas and the simulated degree of wetness was only dependent on terrain location.

The difference in annual runoff for the various grid sizes was much smaller between the three basins than between the two years of simulation (Fig. 6a). Differences between the years in annual spatially and temporally averaged soil moisture were relatively small (Fig. 6b). The average soil water saturation changed rapidly with grid sizes up to 150 m, but very little after that.

The relative deviation, E, of the moisture content was plotted against the grid size (Fig. 7). E is defined as:

$$E = \left| \frac{\theta_i - \theta_0}{\theta_0} \right| \tag{6}$$

where θ_i is the average yearly soil moisture content at scale i and θ_0 is the reference moisture content at 0 m obtained by an extrapolation to a grid size of 0 m using a linear regression of ln θ versus the

grid size (Fig. 6b). The relative deviation in moisture content for a particular scale was almost the same between years and variation in relative deviation between basins became obvious (Fig. 7). The magnitude of the deviation for larger grid sizes was greater for basin 1 (Fig. 1) which has a relatively high percentage of shallow, less well drained soils than basins 2 or 3. The slope of the lines was, initially, about 1.2 (Fig. 7), indicating that the relative deviation increased by a factor of $10^{1.2}$ or 16 when grid size increased from 10 to 100 m.

4. DISCUSSION

The results of the two-factor factorial experiment are summarized in Table 2. One factor represents the map derived from elevation (topography), and the other factor represents the maps from soil type and land use. In the table, the effective precipitation is the difference of the precipitation and the actual evaporation. Both the annual effective precipitation and yearly averaged soil moisture for the whole watershed changed little when the soil type and land use maps were changed from 20 to 200 m while the grid cell size of the topography remained the same (Table 2). For example, for the 20 m grid topography map, the average moisture content for year 1 was 0.798 when the grid spacing for the soil type and land use maps was 20 m, while using a 200 m grid cell size for these two maps (and retaining the topography grid size at 20 m) resulted in an average moisture content of 0.803. Clearly, the actual evaporation is not sensitive to the land use on these shallow soils. In contrast, aggregation of topography from 20 to 200 m had a large effect on model outputs. The change in scale from 20 to 200 m for topography resulted in an increase in the watershed moisture content by nearly 20% in both years and at both the 20 and 200 m scales of the soil type and land use maps. Because

aggregation of topography increased wetness, it increased evapotranspiration and, thereby, decreased the effective precipitation (Table 2).

The spatial moisture distributions on two dates (Fig. 8a) and the average soil moisture contents for three monthly periods (Fig. 8b) were analyzed to assess the scaling effect. These were either in dry or wet periods. The "wet" day, 31 March 1992, had 1.3 cm precipitation in the previous three days while evaporation was small. The "dry" day, 19 June 1992, occurred during a drought period with no rain for the previous 12 days under high evaporative conditions. For monthly average data, August 1991 (dry) was compared with August 1992 and October 1992 which were both wet but with vegetation in different growth stages. In all cases, aggregation caused a dramatic loss in information of moisture content distribution of the soil. During wet periods, Ω decreased 1 to 2 orders of magnitude when grid size changed from 10 to 600 m (Figs. 8a and 8b). The decrease in Ω for increasing grid sizes was less during dry periods than during wet periods but was still substantial. Thus, using a common grid cell size in the USA of 30 m, rather than 10 m for the simulation, results during the wet period caused a loss of information on soil moisture distribution of 50%. For the UK, where the common grid size is 50 m, the information loss was 70%. Since soil moisture is a major factor that controls biological and chemical processes, we infer that simulation of those dynamics at larger grid sizes may overestimate the rate of anaerobic soil processes and the growth rate of the plants. Therefore, we recommend for watershed simulations to use a grid cell size smaller that 30 m and preferably 10 m if the data is available.

As expected, the information index, Ω, for soil type and land use showed only a weak dependence on grid size (Fig. 9a). Also, aggregation did not change the information content of the distribution of grid cell elevations and resulted in only moderate information loss for slope gradient (Fig. 9b). In contrast, aggregation reduced the Ω value of the Laplacian (calculated from the topographic information) by two orders of magnitude (Fig. 9b). Note, that a small Ω value indicates less difference among cells and that the hydrological behavior at high levels of aggregation approximates a uniform area. Thus, the information analysis provides evidence that the aggregation of the topographic data is the source of most aggregation error in the hydrologic simulation; and that much of this error can be attributed to the behavior of the Laplacian. In other words, increasing the grid cell size misrepresents the curvature of the landscape and results in higher moisture contents and decreases the variation in the distribution of moisture content among cells (Fig. 4b).

In the wet periods, the decrease of the Ω value of soil moisture content due to aggregation (Fig. 8) was of the same order as the information loss for the Laplacian distribution (Fig. 9b). This occurs because the moisture content differences during wet periods are caused by lateral water transport (Eqs. (1) and (2)), and this process is dominated by the Laplacian. For dry periods, evaporation is the main factor in moisture loss and lateral transport is small, causing the information loss to be less dependent on the Laplacian than during wet periods (Figs. 8a and 8b).

Figure 9b also explains why soils during a wet period were near saturation in most areas at grid sizes of 400 m (Fig. 5). That is, a large grid size results in a small range of the Laplacian spectrum; and since the amount of water remains approximately the same which has to be transported out of the

watershed, the unsaturated conductivity must compensate for the decrease in driving force as expressed by the Laplacian. Since conductivity depends on moisture content the moisture content increases.

Our unsaturated flow model and its saturated flow counterpart, TOPMODEL, both showed the same sensitivity of scale with respect to the topographic input data. Even more remarkable is that Zhang and Montgomery [1994] found, similarly, for two watersheds with TOPMODEL, that the 10 m grid size provided a substantial improvement over the 30 and 90 m data. Thus, despite the differences, the structure of the models might be more similar than originally anticipated.

5. CONCLUDING REMARKS

Errors introduced by aggregation of spatial input data have important ramifications for the use of GIS-based hydrology models. In this study, deviations from the simulations at the smallest grid size increased proportionally to grid size over the range of scales most commonly used in GIS simulation studies (Fig. 7). This is in agreement with the argument used by Beven [1995] that the aggregation approach towards macro-scale hydrological modeling, using averaged parameter values, was inadequate to represent hydrological processes at a large scale. Thus, a disaggregation approach to developing scale-dependent models is advocated by Beven [1995]. However, the computation cost (CPU time) decreases in proportion with the square of the grid size. Our results, such as represented in Fig. 7, can, at least in the northeastern USA, help guide choice of a grid size which is a compromise between accuracy and computation time in large area simulations.

In this study, we showed that among the several types of input information changes in the scale of topography had the greatest effects on the simulation results. This parallels the results with TOPMODEL [Braun et al., 1997; Zhang and Montgomery, 1994]. Aggregation had, especially, a large effect during wet periods. The scale of topography is critical because hydrological behavior is driven by the first derivative (slope gradient) and the second derivative (Laplacian or slope curvature) of the elevation data. The information of the Laplacian has the same response to grid size as the relative error in the simulation of the moisture content (Figs. 7 and 8). Thus, the Laplacian Ω value can provide an *a priori* estimate of the magnitude of the deviation in soil moisture content values created by aggregation, and can aid in deciding the optimum grid-scale for simulating the hydrology of large areas.

ACKNOWLEDGMENTS

This research was supported by the Agricultural Ecosystems Program at Cornell University funded by the United States Department of Agriculture.

REFERENCES

Ambroise, B., K. Beven, and J. Freer. 1996. Toward a generalization of the TOPMODEL concepts. Topographic indices of hydrological similarity. Water Resources Research 32:2135-2145.

Baveye, P. 1997. Scaling spatial predictability. Can it be done without considering the natural scales of processes? Joint AGU Chapman/SSSA Outreach Conferences on Application of GIS, Remote Sensing, Geostatistics, and Solute Transport Modeling to the Assessment of Non-point Source Pollutants in the Vadose Zone. Riverside, CA. October 19-24, 1997.

Beven, K.J. 1986. Hillslope runoff processes and flood frequency characteristics. In: Hillslope Processes, A.D. Abrahams, Editor. Allen and Unwin, Boston, MA. pp. 187-202.

Beven, K.J. 1995. Linking parameters across scales - subgrid parameterizations and scale dependent hydrological models. Hydrological Processes 9:507-525.

Beven, K.J. and M.J. Kirkby. 1979. A physically-based variable contributing area model of basin hydrology. Hydrological Sciences Bulletin 24:43-69.

Braun, P., T. Molnar, and H.B. Kleeberg. 1997. The problem of scaling in grid-related hydrological process modelling. Hydrological Processes 11:1219-1230.

Bruneau, P., C. Gascuel-Odoux, P. Robin, Ph. Merot, and K. Beven. 1995. Sensitivity to space and time resolution of a hydrological model using digital elevation data. Hydrological Processes 9:69-81.

Burrough, P.A. 1996. Opportunities and limitation of GIS-based modeling of solute transport at the regional scale. In: Applications of GIS to the Modeling of Non-Point Source Pollutants in the Vadose Zone, D.L. Corwin and K. Loague, Editors. SSSA Special Publication, Soil Science Society of America, Madison, WI.

CERL. 1993. Geographic Resources Analysis Support System, Version 4.1. User's Reference Manual. Construction Engineering Research Laboratory, U.S. Army, Champaign, IL.

Cornell University Department of Geology. 1959. Geology of the Cayuga Lake Basin: A Guide for the 31st Annual Field Meeting of the New York State Geological Association. Cornell University, Ithaca, NY.

Dunne, T. 1978. Field studies of hillslope flow processes. In: Hillslope Hydrology, M.J. Kirkby, Editor. John Wiley and Sons, New York, NY. pp. 227-289.

Fisher, P., R.J. Abrahart, and W. Herbinger. 1997. The sensitivity of two distributed non-point source pollution models to the spatial arrangement of the landscape. Hydrological Processes 11:241-252.

Frankenberger, J.R., E.S. Brooks, M.T. Walter, M.F. Walter, and T.S. Steenhuis. 1998. A GIS-based variable source area hydrology model. Hydrological Processes. In Press.

Haith, D.A. and L.L. Shoemaker. 1987. Generalized watershed loading functions for stream flow nutrients. Water Resources Bulletin 23:471-478.

Kuo, W.-L., P. Longabucco, M.R. Rafferty, J. Boll, and T.S. Steenhuis. 1996. An integrated GIS-based model for soil water and nitrogen dynamics in a New York City watershed. Proc. AWRA Symposium on Watershed Restoration Management. Syracuse, NY. July 14-17, 1966. pp. 17-26.

Moore, I.D., R.B. Grayson, and A.R. Lanson. 1991. Digital terrain modelling: A review of hydrological, geomorphological, and biological applications. Hydrological Processes 5:3-30.

Moore, I.D., A. Lewis, and J.C. Gallant. 1993. Terrain attributes: Estimation methods and scale effects. In: Modelling Change in Environmental Systems, A.J. Jakeman, M.B. Beck, and McAleer, Editors. John Wiley and Sons, New York, NY.

Mitasova, H., L. Mitas, W.M. Brown, D.P. Gerdes, I. Kosinovsky, and T. Baker. 1995. Modelling spatially and temporally distributed phenomena: new methods and tools for GRASS GIS. International Journal Geographical Information Systems 9:433-446.

Neeley, J.A. 1965. Soil Survey of Tompkins County, NY. U.S. Department of Agriculture - Soil Conservation Service. U.S. Government Printing Office, Washington, DC.

Neter, J., M.L. Kutner, C.J. Nachtsheim, and W. Wasserman. 1996. Applied Linear Statistical Models. 4th edition. Irwin, Chicago, IL.

Owensby, J.R. and D.S. Enzell. 1992. Climatology of the U.S. No. 81. Monthly Station Normals of Temperature, Precipitation, and Heating and Cooling Degree Days 1961-1990, New York. National Climatic Data Center, Asheville, NC.

Poiani, K.A., B.L. Bedford, and M.D. Merrill. 1996. A GIS-based index for relating landscape characteristics to potential nitrogen leaching in wetlands. Landscape Ecology 11:237-255.

Quinn, P., K. Beven, P. Chevallier, and O. Planchon. 1991. The prediction of hillslope flow paths for distributed hydrological modeling using digital terrain models. Hydrological Processes 5:59-79.

Shannon, C.E. and W. Weaver. 1949. The Mathematical Theory of Communication. University of Illinois Press, Urbana, IL.

Singh, V.P. 1997. The use of entropy in hydrology and water resources. Hydrological Processes 11:587-626.

Star, J., and J. Estes. 1990. Geographic Information Systems: An Introduction. 2nd Edition. Prentice Hall, Englewood Cliffs, NJ.

Star, J.L., J.E. Estes, and K.C. McWire. 1997. Integration of Geographic Information Systems and Remote Sensing. Cambridge University Press, Cambridge, NJ.

Steenhuis, T.S. and W.H. van der Molen. 1986. The Thornthwaite-Mather procedure as a simple engineering method to predict recharge. Journal of Hydrology 84:221-229.

Steenhuis, T.S., T.L. Richard, M.B. Parlange, S.A. Aburime, L.D. Geohring, and J.-Y. Parlange. 1988. Preferential flow influences on drainage of shallow sloping soils. Agricultural Water Management 14:137-151.

Steenhuis, T.S., M. Winchell, J. Rossing, J.A. Zollweg, and M.F. Walter. 1995. SCS runoff equation revisited for variable-source runoff areas. ASCE Journal of Irrigation and Drainage 121(3):234-238.

Swaney, D.P., W.-L. Kuo, D.A. Weinstein, C. Mohler, S. DeGloria, C. Pelkie, F. Tsai, T.S. Steenhuis, and C.E. McCulloch. 1996. Response of a watershed model to varying spatial landscape characteristics. In: Proc. Spatial Accuracy Assessment in Natural Resources and Environmental Sciences: Second International Symposium, H.T. Owrer, R.L. Czaplewski, and H. Hammre, Editors. Fort Collins, CO. May 21-23, 1996. pp. 65-72.

USEPA. 1994. National Water Quality Inventory, 1992 Report to Congress. Office of Water, U.S. Environmental Protection Agency, Washington, DC.

USEPA. 1995. National water quality inventory, 1994 Report to Congress. EPA841-R-95-006. Office of Water, U.S. Environmental Protection Agency, Washington, DC.

USEPA. 1996. Why Watersheds? EPA800-F-96-001. Office of Water, U.S. Environmental Protection Agency, Washington, DC.

Vieux, B.E. 1993. Aggregation and smoothing effects on surface runoff modeling. ASCE Journal of Computing in Civil Engineering 7:310-338.

Wolock, D.M. and C.V. Price. 1994. Effects of digital elevation model map scale and data resolution on topography-based watershed model. Water Resources Research 30:3041-3052.

Zhang, W. and D.R. Montgomery. 1994. Digital elevation model grid size, landscape representation, and hydrologic simulations. Water Resources Research 30:1019-1028.

Zollweg, J.A., W.J. Gburek, and T.S. Steenhuis. 1996. SMoRMod - A GIS-integrated rainfall-runoff model applied to a small northeast U.S. watershed. Trans. ASAE 39:1299-1307.

Table 1. Summary information for three basins.

	Basin 1	Basin 2	Basin 3
Area (ha)	647	2360	742
Topography			
elevation range (m)	317 - 433	335 - 561	317 - 488
slope gradient range (%)	0 - 44	0 - 59	0 - 35
Soil Type			
(% of basin area)			
1. Well drained	87	79	61
2. Poorly drained	13	21	39
Land Use			
(% of basin area)			
1. Permanent vegetation (forest and wetland)	47	41	34
2. Crop Land	39	43	50
3. Grass	6	10	8
4. Urban	8	6	8

Table 2. The results of a two factor experiment: Topography vs. soil type and land use with two levels of 20 and 200 m.

A. Year 1 runoff, mm

		Topography	
		20 m	200 m
Soil type & Land use	20 m	483	481
	200 m	481	491

Year 2 runoff, mm

		Topography	
		20 m	200 m
Soil type & Land use	20 m	258	189
	200 m	254	201

B. Year 1 averaged soil moisture

		Topography	
		20 m	200 m
Soil type & Land use	20 m	0.798	0.972
	200 m	0.803	0.968

Year 2 averaged soil moisture

		Topography	
		20 m	200 m
Soil type & Land use	20 m	0.726	0.918
	200 m	0.729	0.905

C. Year 1 effective precipitation, mm

		Topography	
		20 m	200 m
Soil type & Land use	20 m	500	450
	200 m	498	457

Year 2 effective precipitation, mm

		Topography	
		20 m	200 m
Soil type & Land use	20 m	233	159
	200 m	229	172

FIGURE TITLES

Figure 1. Location, soil type and land use maps of the study area, a subcatchment of the Fall Creek in central New York.

Figure 2. An example of spatial aggregation of a catchment from grid cell $L = l$ to large grid cell $L = 3\,l$. The area inside the watershed at the fine scale, $L = l$, is shown in gray. Catchment size after aggregation = $(6/9 + 3/9 + 2/9 + 2/9) * L^2 = 13 * l^2$.

Figure 3. Information index (Ω) of slope (∇h) and Laplacian ($\nabla^2 h$) vs. number of bins at cell sizes of 50, 200, and 600 m.

Figure 4. Monthly simulation results for the whole catchment of total area at cell sizes of 10, 30, 50, 100, and 400 m: (a) cumulative monthly runoff, (b) monthly average soil moisture, and (c) cumulated monthly effective precipitation. Legends are shown in Fig. 4a.

Figure 5. Spatial simulation soil moisture for a selected sample date, 3/31/93, at cell sizes of 10, 30, 50, 100, and 400 m.

Figure 6. Simulation results of three basins in year 1 and year 2: (a) annual runoff, and (b) yearly average soil moisture. Legends are shown in Fig. 6a.

Figure 7. Relative results of yearly average soil moisture for two years in the three basins. The dashed line is year 1 and the solid line is year 2. Symbols indicate basins and are shown in legend.

Figure 8. Information index (Ω) vs. grid size δ for soil moisture distribution: (a) at two sample dates, and (b) at monthly average soil moisture distribution at eight chosen months over the study period. Solid lines represent wet period and dashed lines represent dry period.

Figure 9. Information index (Ω) vs. grid size δ for: (a) soil type and land use, and (b) elevation, slope and Laplacian.

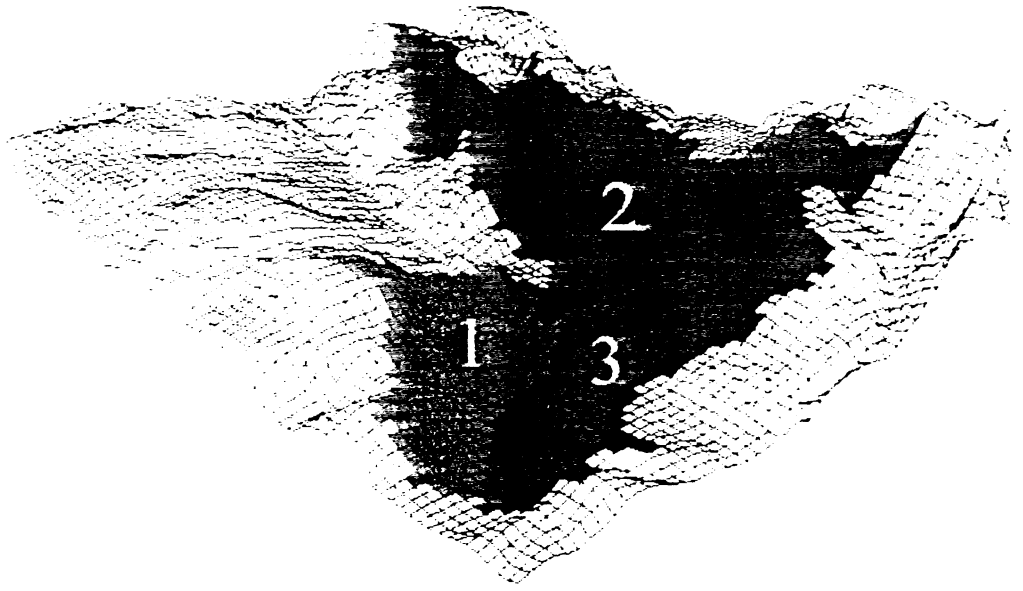
2
1
3

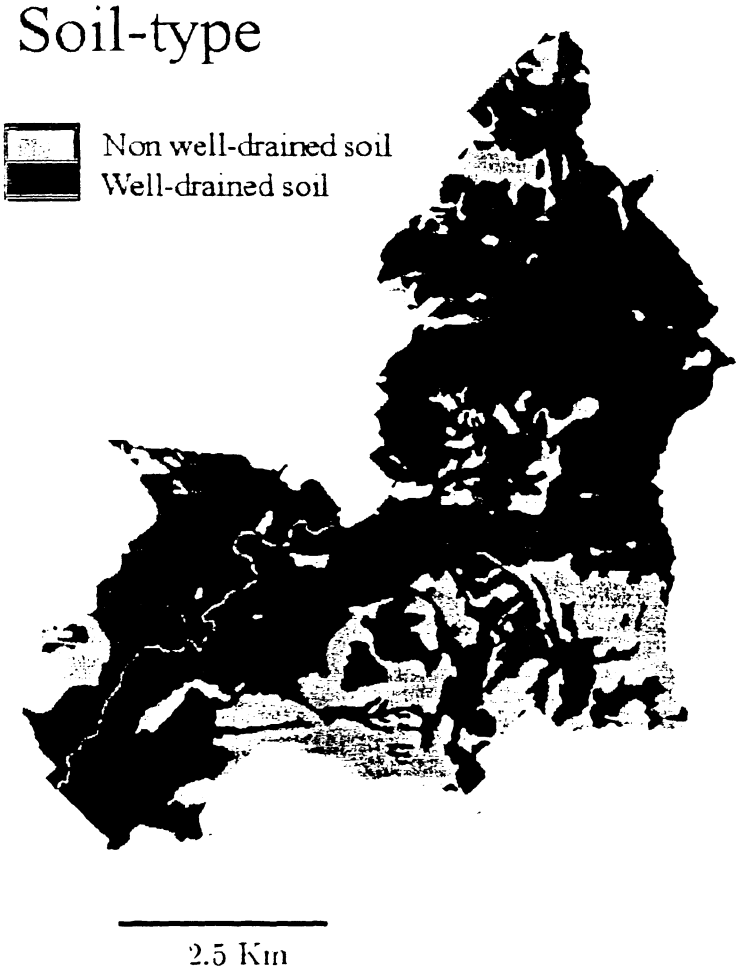
Soil-type
Non well-drained soil
Well-drained soil
2.5 Km

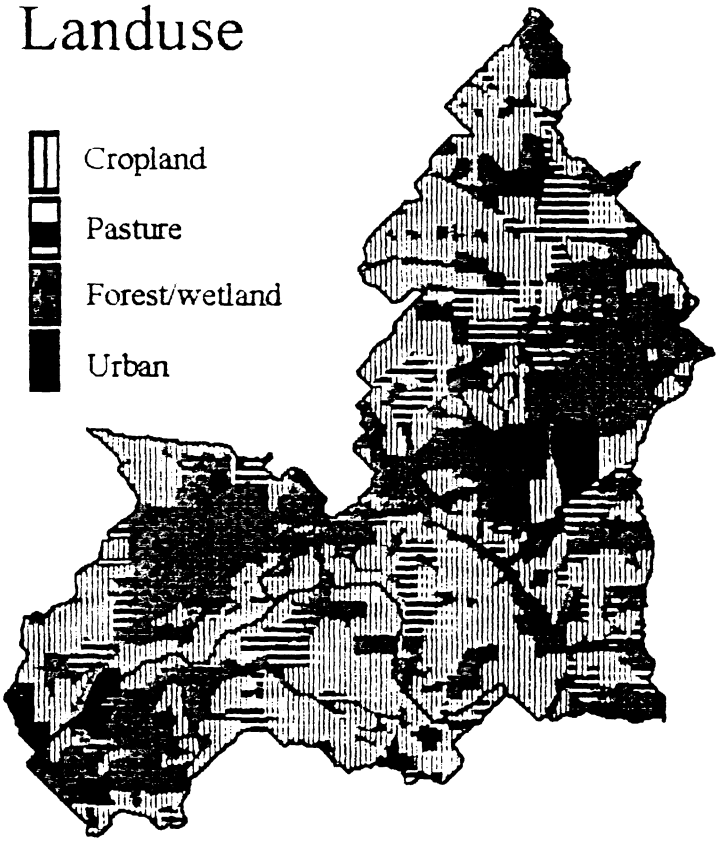
Landuse
Cropland
Pasture
Forest/wetland
Urban

fig 1

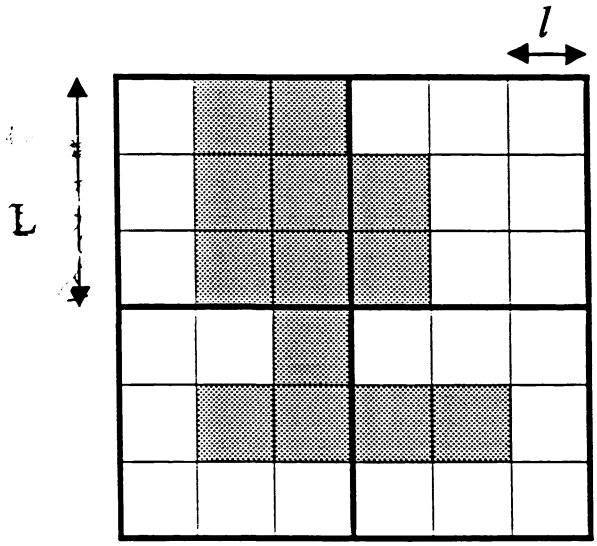

Catchment Area $=13l^2$

Basin-area

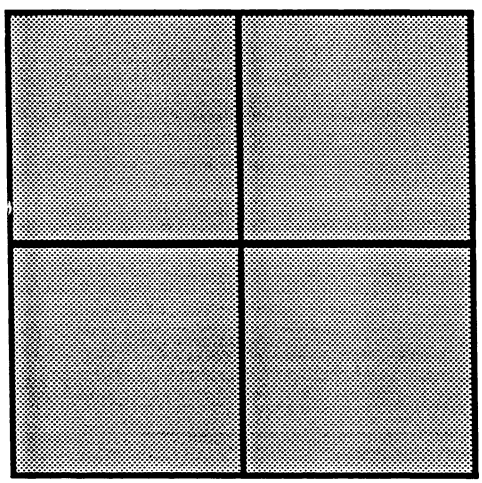

A_p

$\frac{6}{9}$	$\frac{2}{9}$
$\frac{3}{9}$	$\frac{2}{9}$

fig 2

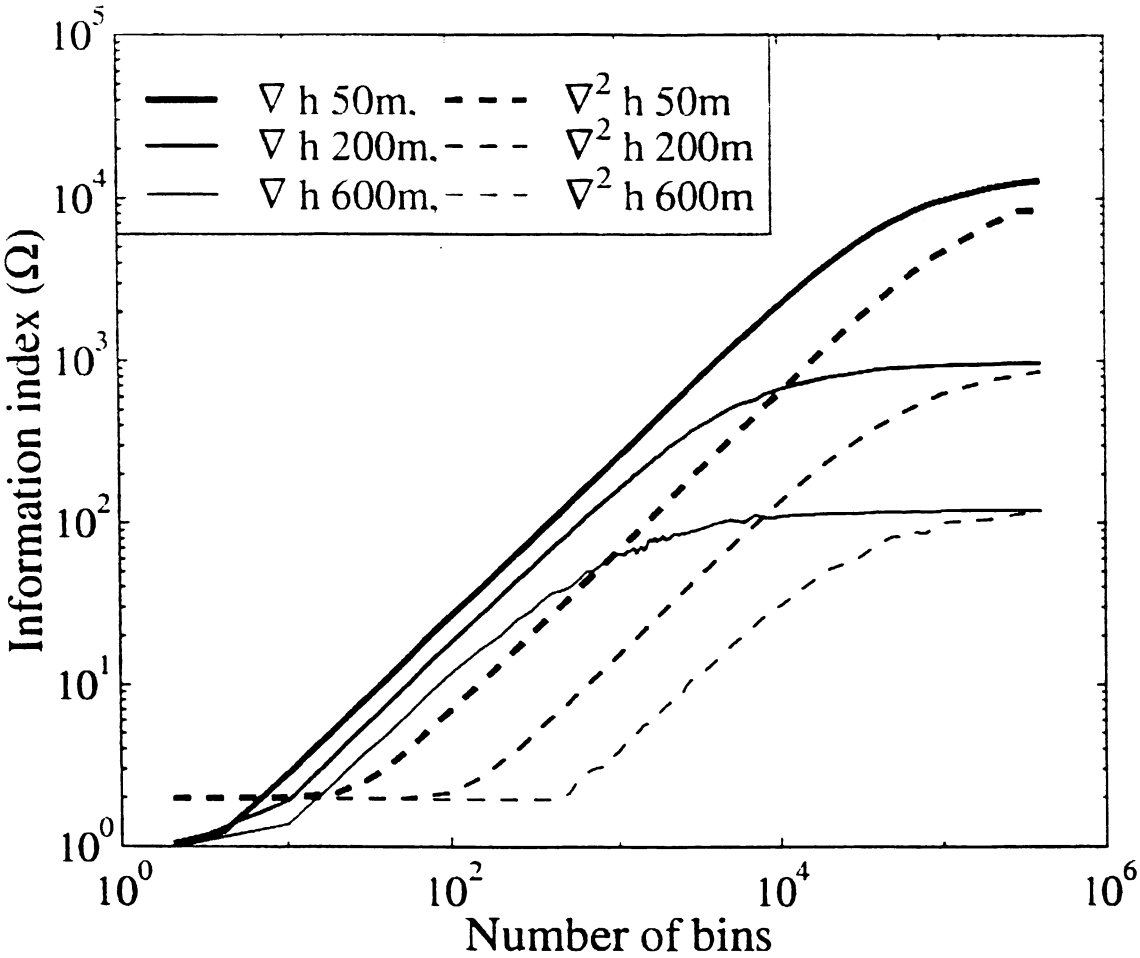
∇ h 50m.
∇ h 200m.
∇ h 600m.
∇² h 50m
∇² h 200m
∇² h 600m
Information index (Ω)
Number of bins
10^0
10^1
10^2
10^3
10^4
10^5
10^6

Fig 3

(a)

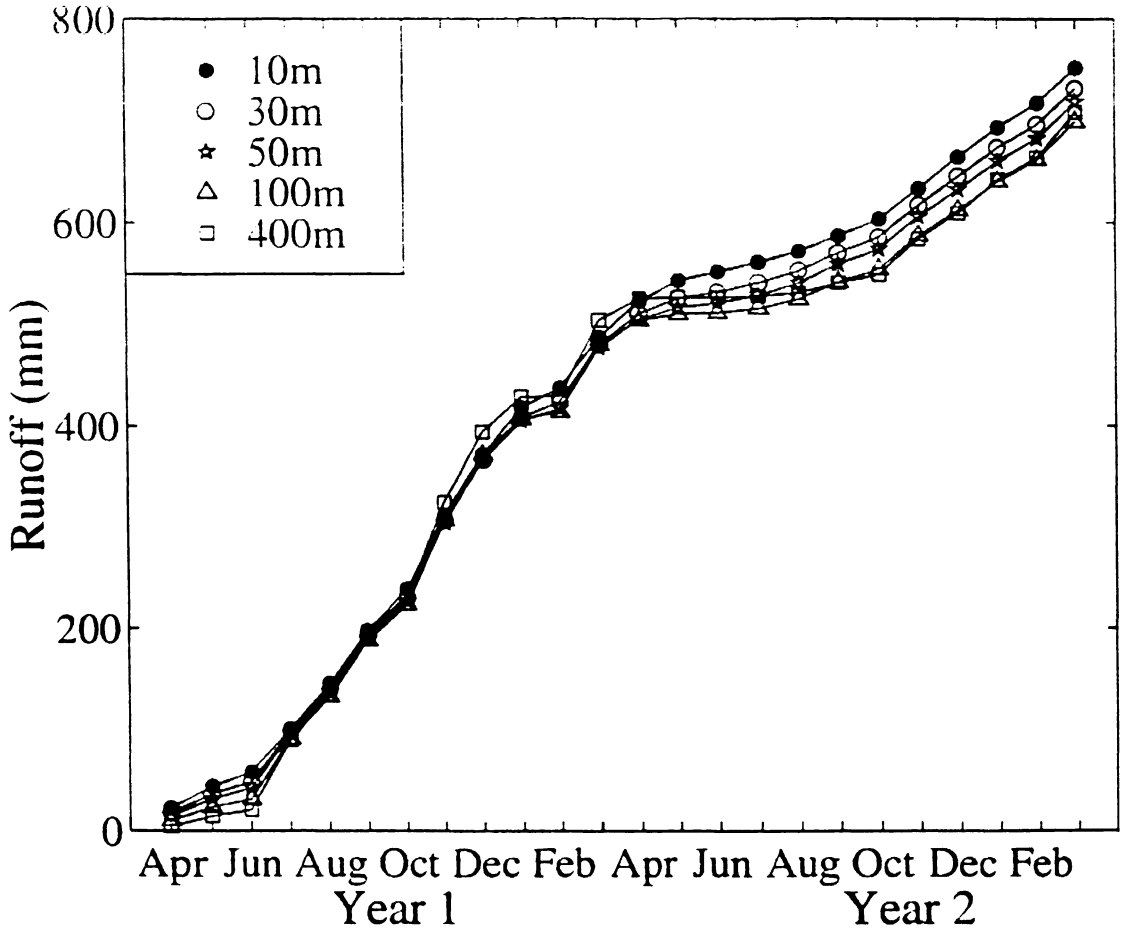
800
600
400
200
0
Runoff (mm)
10m
30m
50m
100m
400m
Apr Jun Aug Oct Dec Feb Apr Jun Aug Oct Dec Feb
Year 1
Year 2

fig 4a

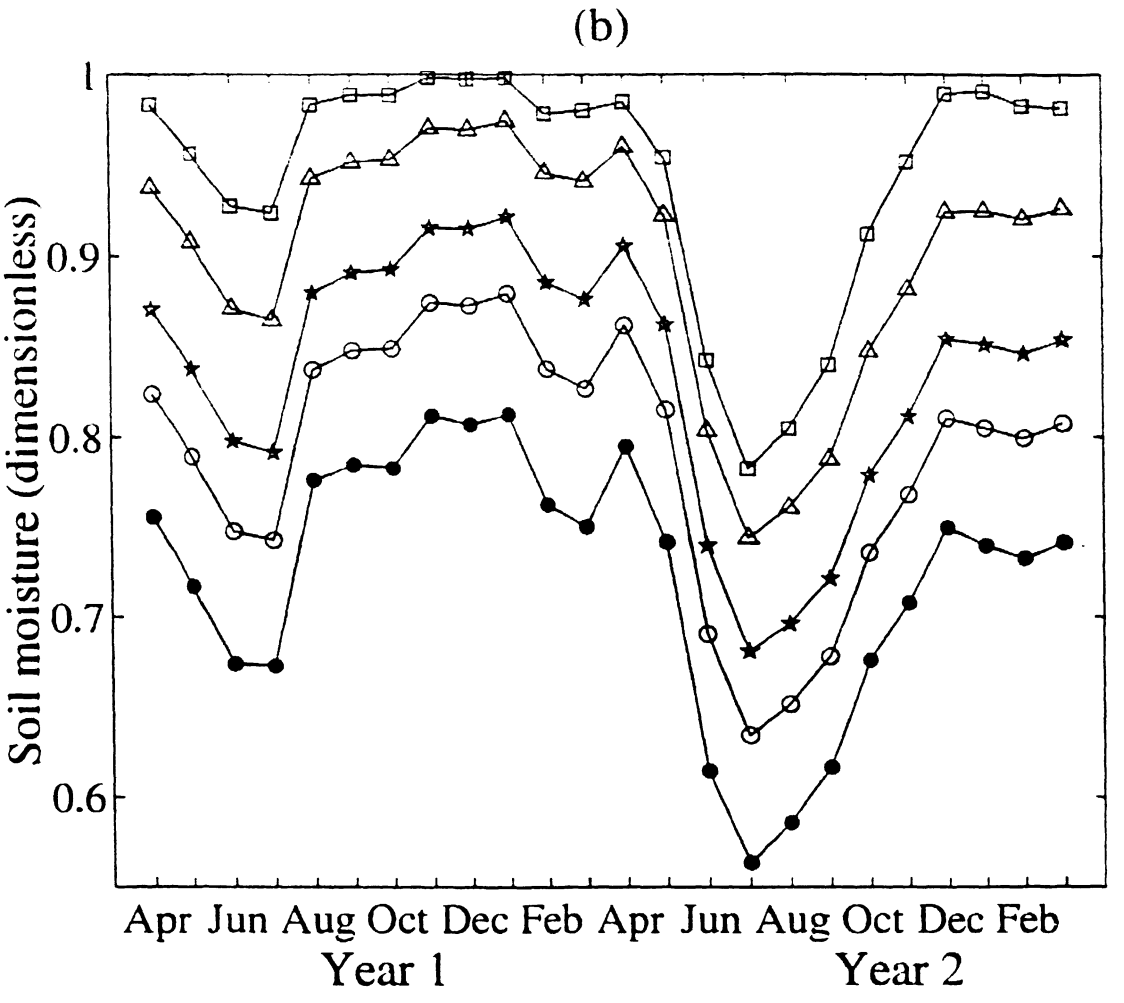
(b)
Soil moisture (dimensionless)
1
0.9
0.8
0.7
0.6
Apr Jun Aug Oct Dec Feb Apr Jun Aug Oct Dec Feb
Year 1
Year 2

fig 4-b

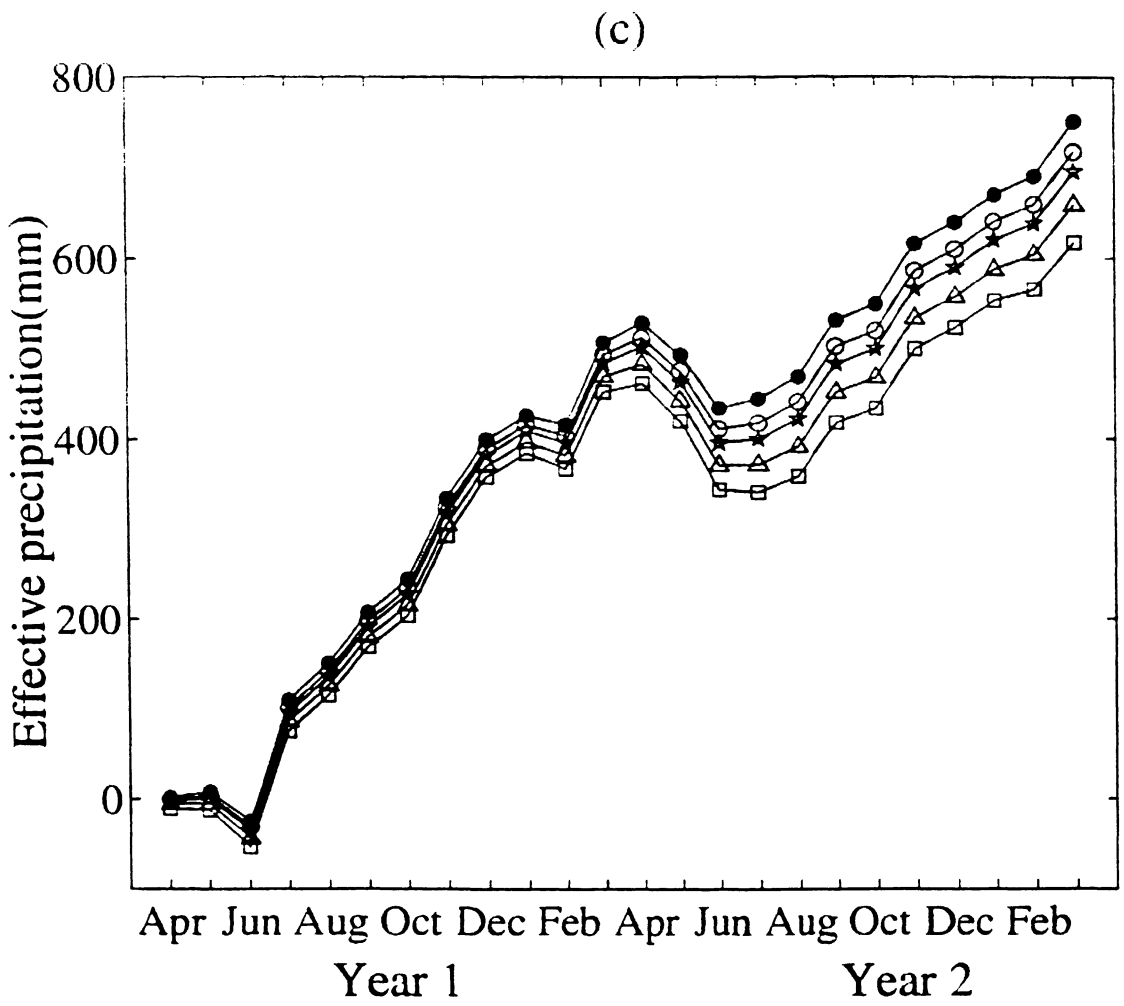
(c)
800
600
400
200
0
Effective precipitation(mm)
Apr Jun Aug Oct Dec Feb Apr Jun Aug Oct Dec Feb
Year 1
Year 2

fig 4c

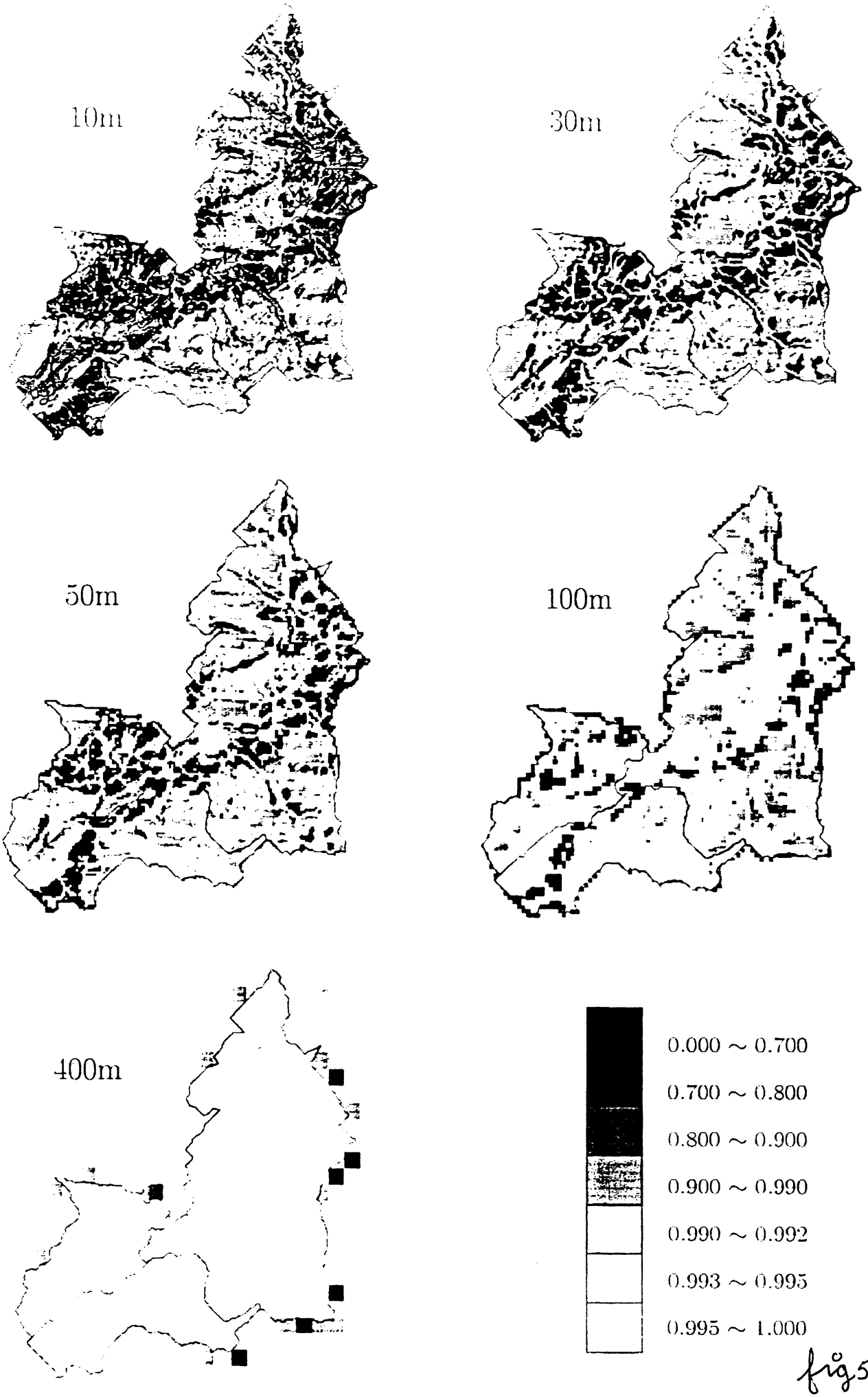
10m
30m
50m
100m
400m
0.000 ~ 0.700
0.700 ~ 0.800
0.800 ~ 0.900
0.900 ~ 0.990
0.990 ~ 0.992
0.993 ~ 0.995
0.995 ~ 1.000

fig5

(a)

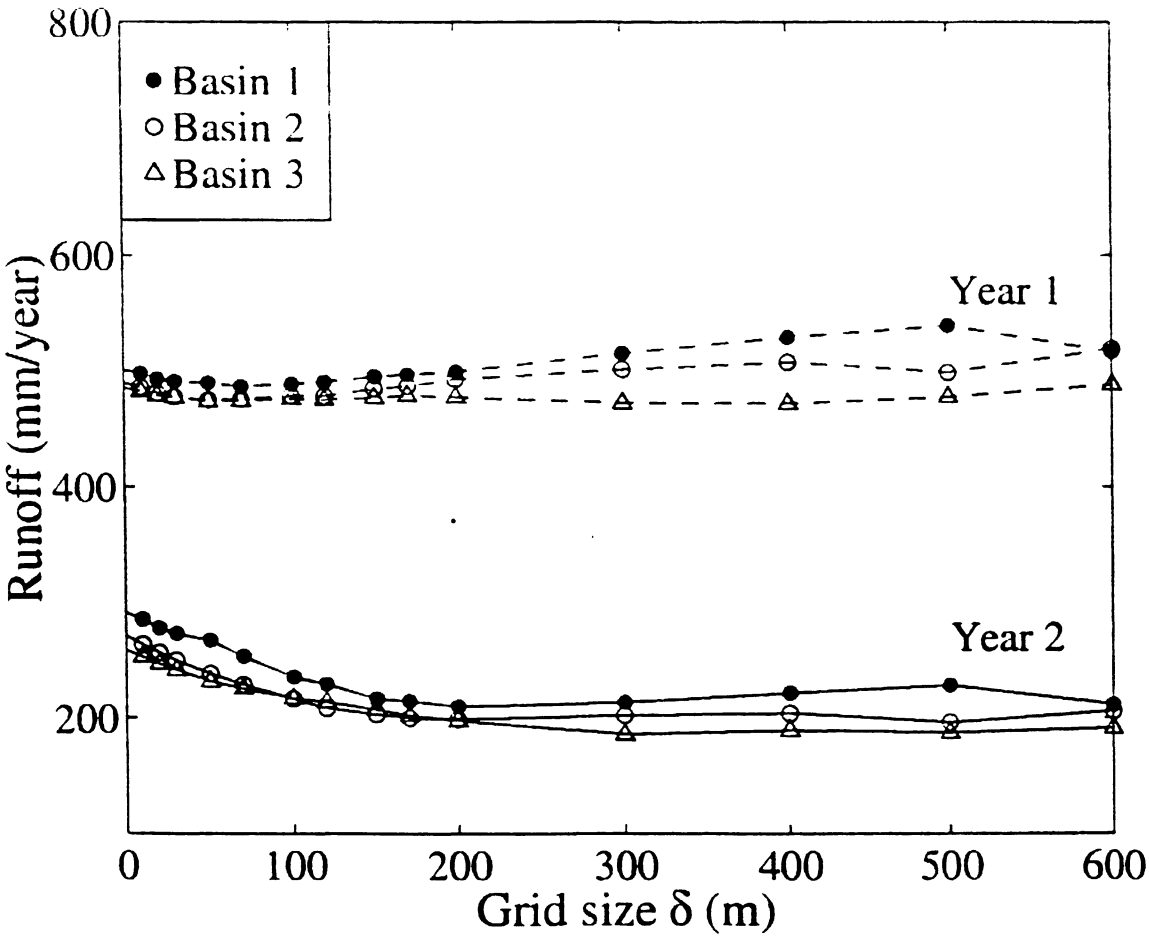
800
600
400
200
Runoff (mm/year)
Basin 1
Basin 2
Basin 3
Year 1
Year 2
0
100
200
300
400
500
600
Grid size δ (m)

fig 6a

(b)

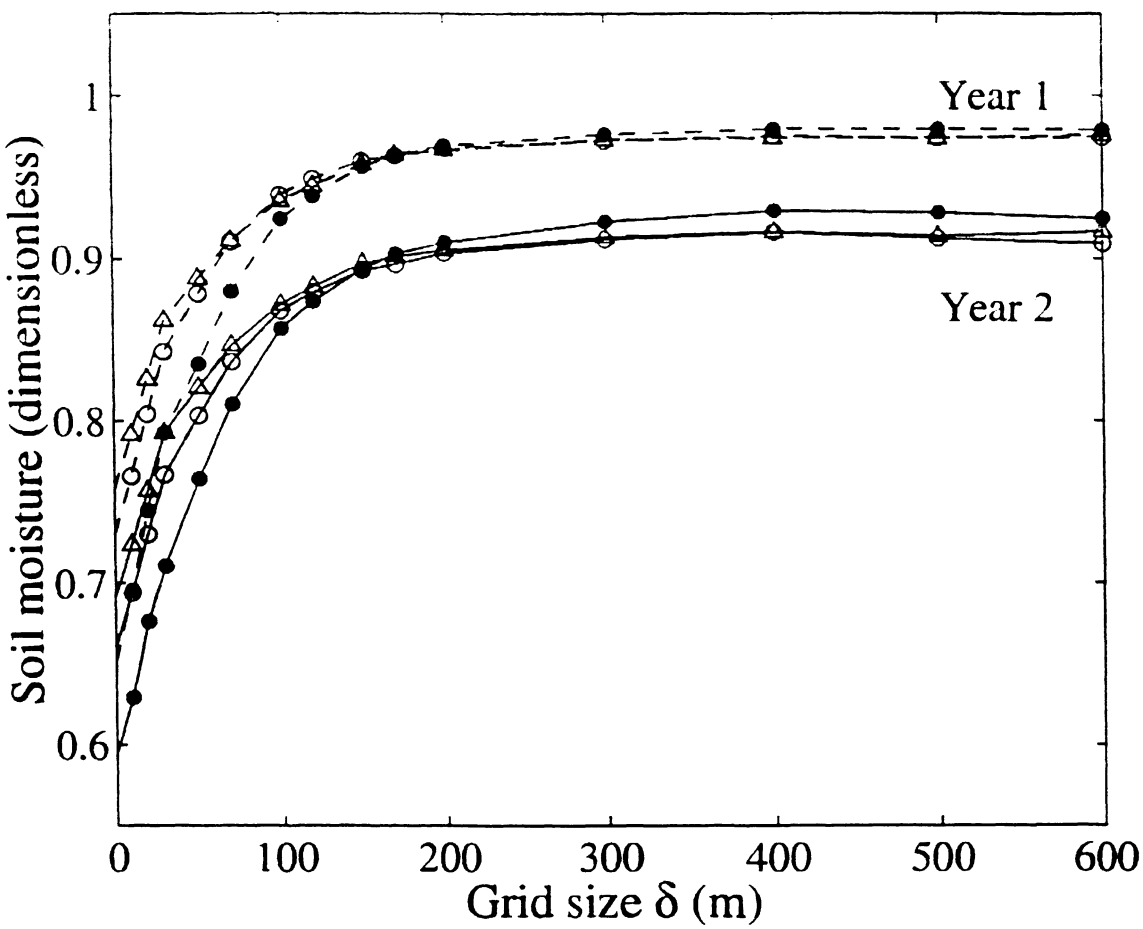
Year 1
Year 2
Soil moisture (dimensionless)
Grid size δ (m)
1
0.9
0.8
0.7
0.6
0
100
200
300
400
500
600

fig 6b

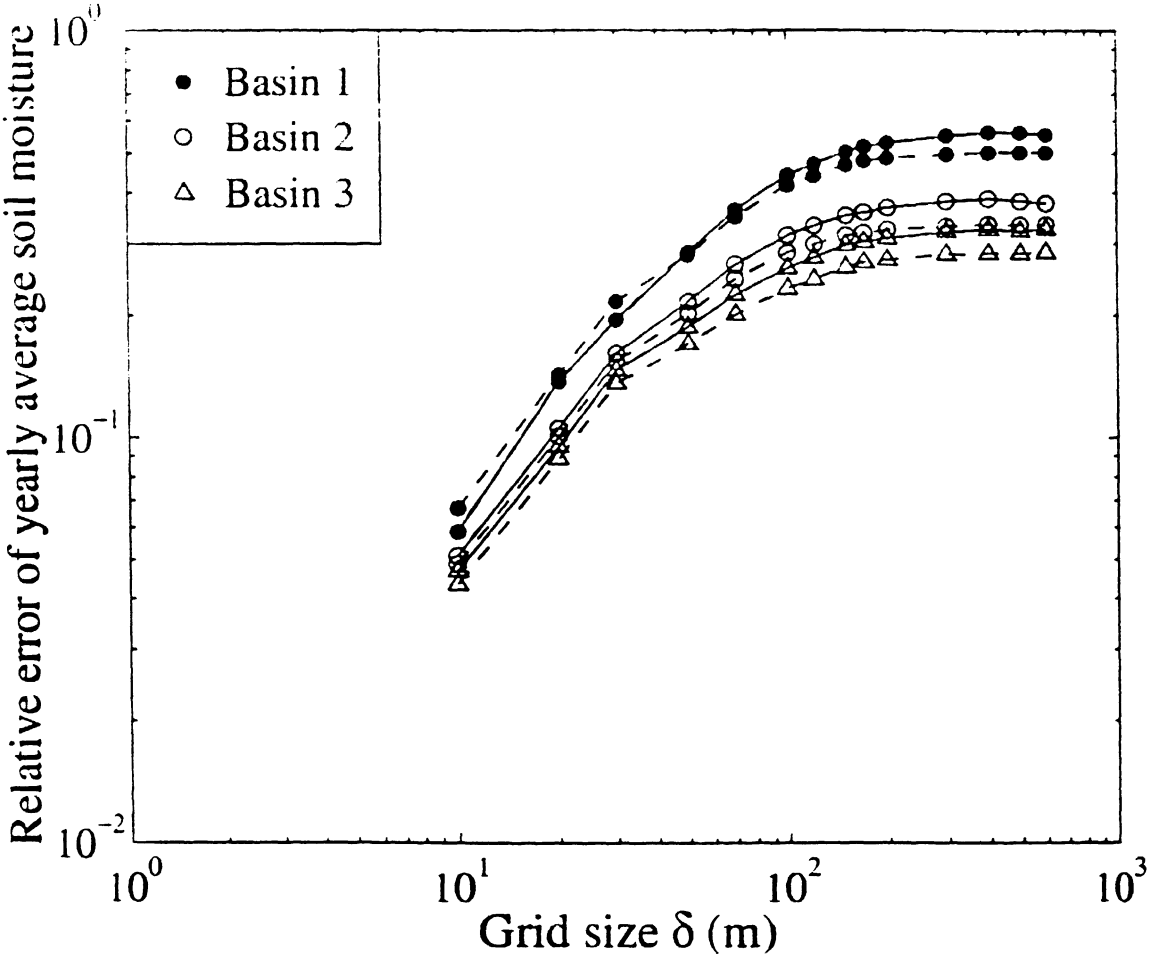
Basin 1
Basin 2
Basin 3
Relative error of yearly average soil moisture
10^{0}
10^{-1}
10^{-2}
10^{0}
10^{1}
10^{2}
10^{3}
Grid size δ (m)

fig 7

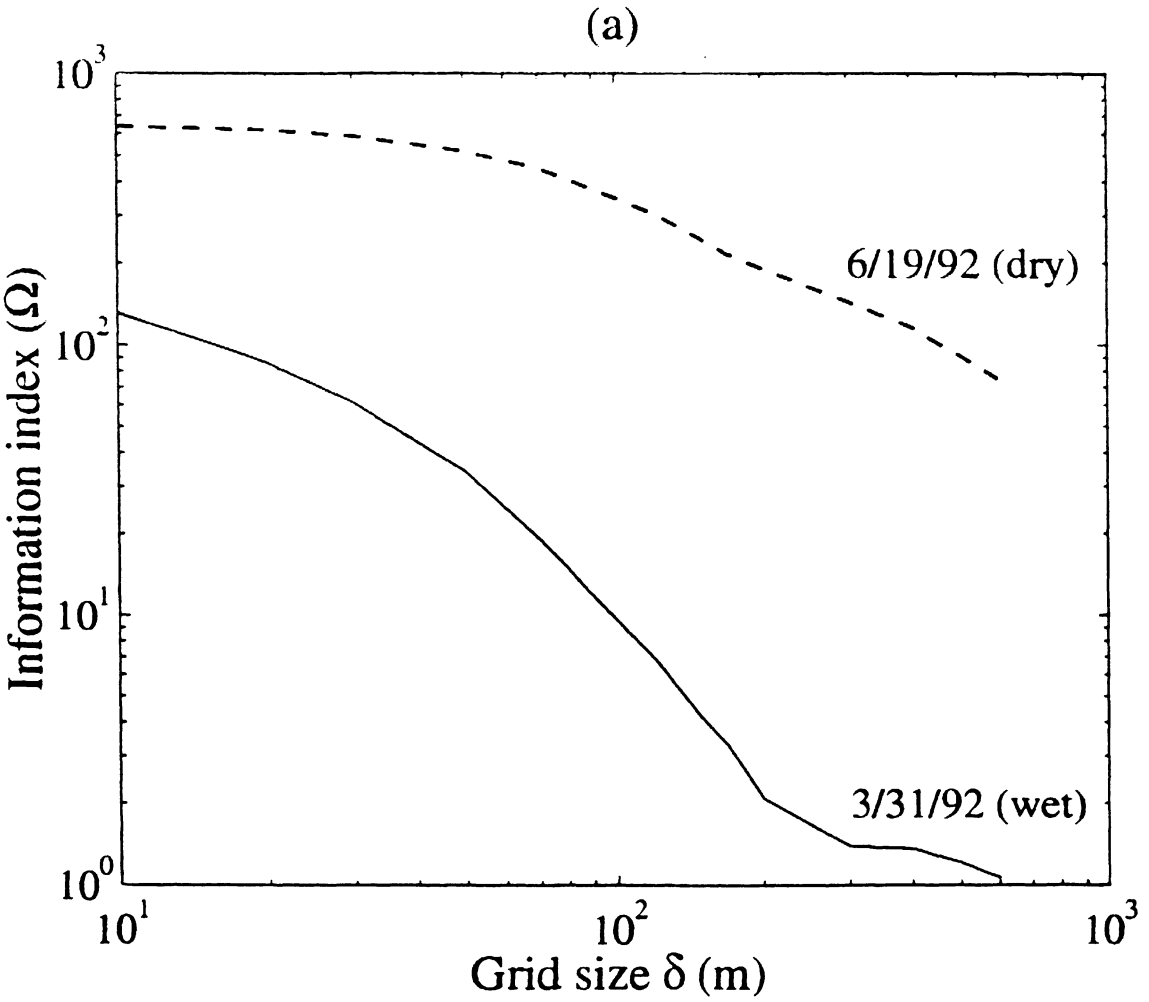
(a)
10^3
10^2
10^1
10^0
Information index (Ω)
6/19/92 (dry)
3/31/92 (wet)
10^1
10^2
10^3
Grid size δ (m)

fig 8a

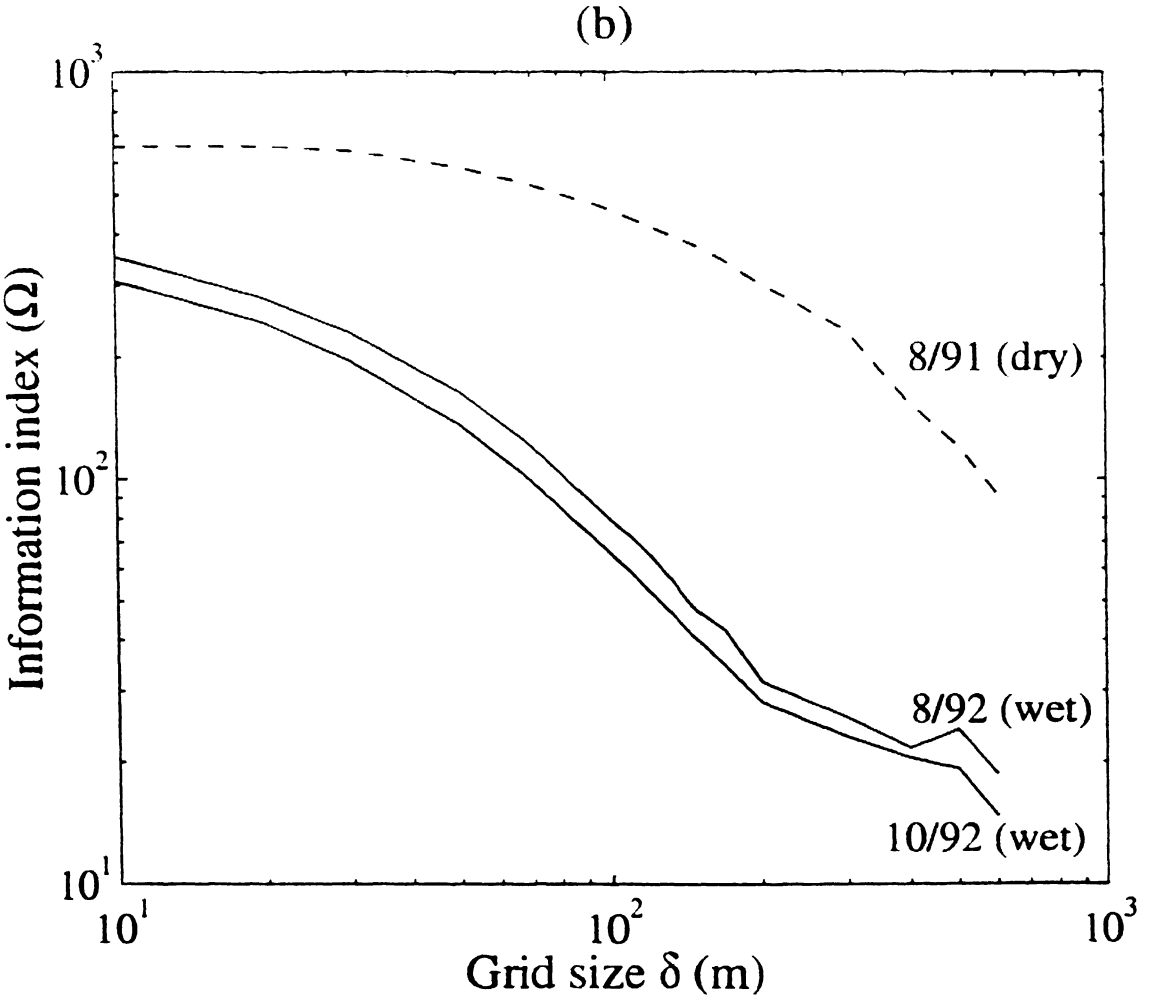
(b)
Information index (Ω)
10^3
10^2
10^1
8/91 (dry)
8/92 (wet)
10/92 (wet)
10^1
10^2
10^3
Grid size δ (m)

fig 8b

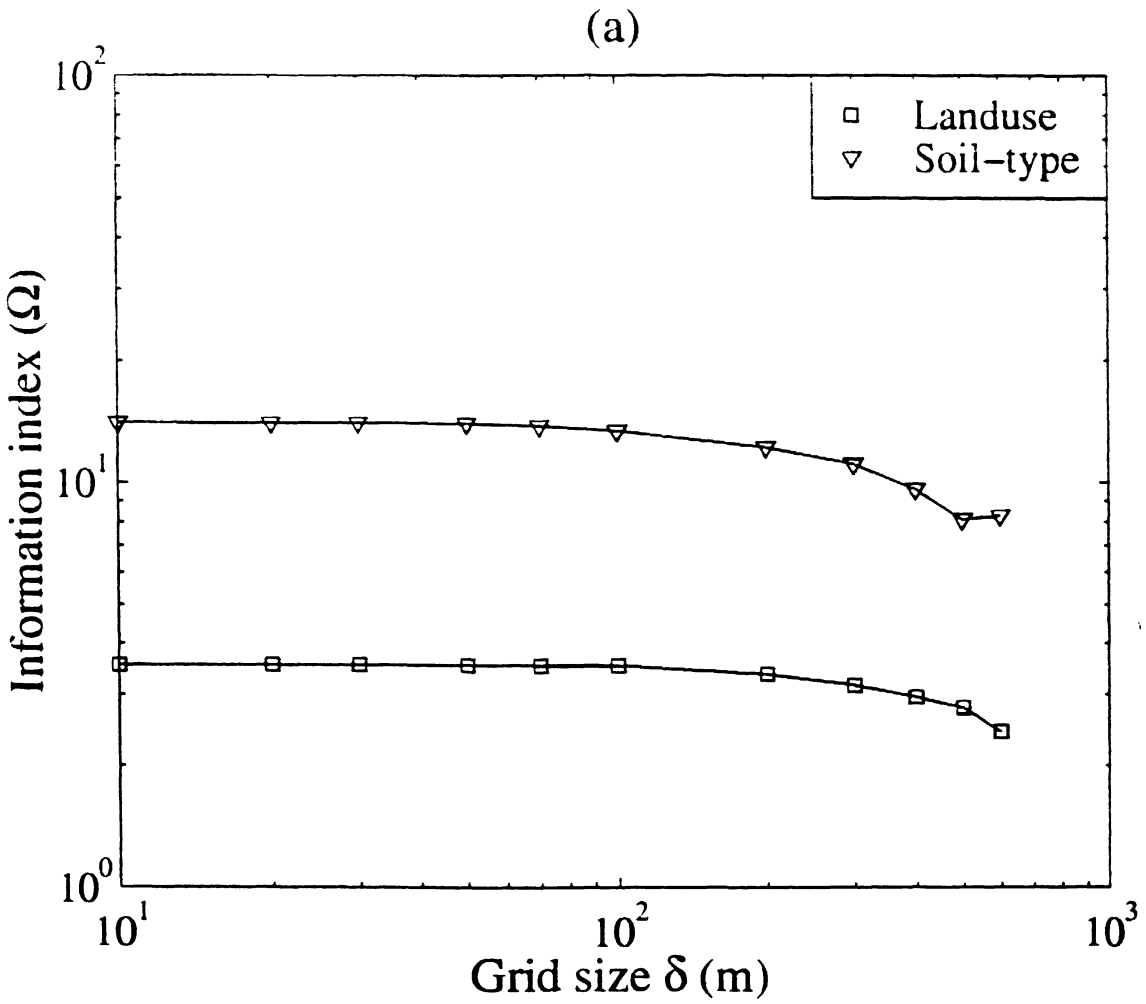
(a)
Landuse
Soil–type
Information index (Ω)
Grid size δ (m)
10^2
10^1
10^0
10^1
10^2
10^3

fig 9a

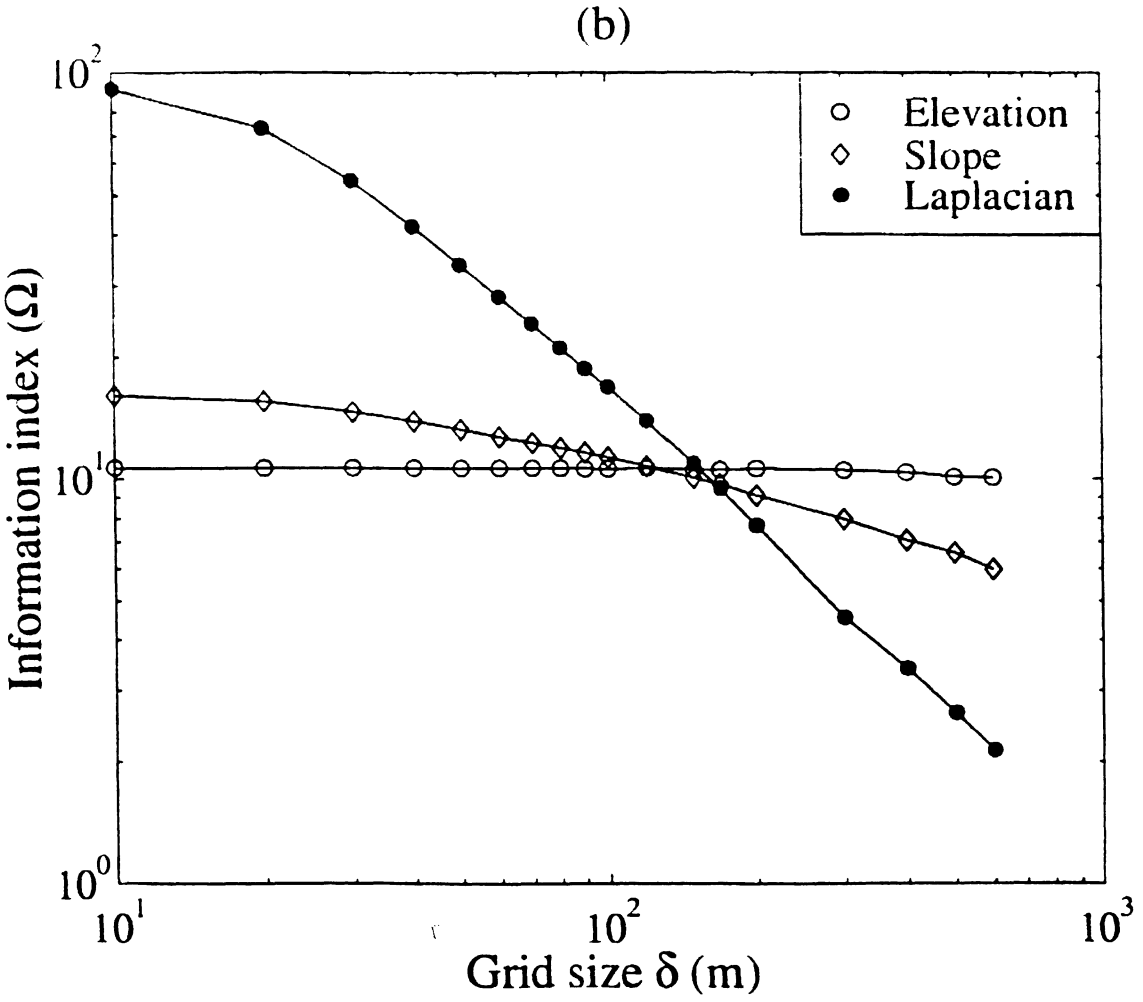
(b)
Elevation
Slope
Laplacian
Information index (Ω)
Grid size δ (m)
10^0
10^1
10^2
10^3

fig 9b